

Transport properties of semiconductor-superconductor junctions in quantizing magnetic fields

Y. Takagaki

NTT Basic Research Laboratories, Atsugi, Kanagawa 243-01, Japan

(Received 25 July 1997; revised manuscript received 28 August 1997)

We present the results of a numerical calculation on the quantum transport properties in junctions of a two-dimensional electron gas and a superconductor in the presence of a perpendicular magnetic field. The low-field conductance drops in a steplike manner, whenever the Landau levels are depopulated, provided that quasiparticle excitations are almost perfectly Andreev reflected from the interface. If the normal reflection is enhanced, the conductance exhibits a sinusoidal oscillation. In contrast to the behavior in conventional conductors, the maxima of the oscillation take place at the depopulation thresholds. In high magnetic fields, a periodic transmission resonance with a complete disappearance of the conductance is found, irrespective of the Andreev-reflection probability. The current distribution indicates that this high-field oscillation is ascribed to the skipping orbit along the interface. We show that the plateau value in the Hall resistance remains unchanged when one of the leads is replaced by the superconductor. Using the selective edge-state detection technique, the distribution of Andreev-reflected quasiparticles among the edge states can be evaluated.

[S0163-1829(98)00107-6]

I. INTRODUCTION

Transport properties in ultrasmall normal-conductor–superconductor (NS) junctions have attracted a great deal of attention in recent years. At low temperatures, the phase information of quasiparticle excitations is preserved during their traversal in the NS system, giving rise to quantum interference effects in the conductance.¹ In addition, the transport can be made ballistic by employing a high-mobility two-dimensional electron gas (2DEG) confined in semiconductor heterostructures as the normal conductor.² Many of the novel characteristics in the NS system originate from the unusual reflection, known as the Andreev reflection, of the quasiparticles from the NS interface.³ An electronlike excitation with energy ε below the Fermi level is reflected as a holelike excitation with energy ε above the Fermi level. The Andreev-reflected quasiparticle exactly follows the trajectory of the original quasiparticle (retroproperty). Moreover, the phase shift associated with the electronlike excitation and the holelike excitation cancels out in the Andreev-reflected trajectory. As pointed out by Beenakker,⁴ the transport properties in the NS system are determined solely by the scattering characteristics of the quasiparticles in the normal region if the Andreev reflection is perfect. This significantly simplifies the theoretical calculation.

In real devices, however, the quasiparticles experience a considerable amount of normal reflection. The Andreev-reflection probability approaches unity when the amplitude of the pair potential Δ is much smaller than the Fermi energy μ .³ However, the difference in μ in the normal conductor and the superconductor, and also a potential barrier at the NS interface,⁵ cause the normal reflection. Additional features may be anticipated to emerge when the partially normal reflection is made possible.⁶ The phase cancellation breaks down when the retroproperty is disrupted by applying a bias to the NS junction. The interference between the electron and hole channels induced by the normal reflection was found to produce a transmission resonance when the bias

approaches the superconducting gap.⁷

In the presence of a magnetic field B applied perpendicular to the 2DEG, the retroproperty is also disturbed since the effective direction of B acting on the quasiparticles is opposite for the electronlike and holelike excitations. The deflection of the ballistic trajectories by the magnetic field was demonstrated in recent experiments.² Since the superconductivity is destroyed if the magnetic field is strong, previous studies on the magnetic-field effect were restricted to weak fields. However, a recent experiment reports that the Josephson coupling in a superconductor-2DEG-superconductor junction can be intact even at $B \sim 8$ T by employing NbN as the superconductor.⁸

In this paper, we investigate the conductance of NS junctions when the in-plane motion of the quasiparticles is Landau quantized. We find that magnetotransport properties depend significantly on the Andreev-reflection probability. When the Andreev reflection is almost perfect, the two-terminal conductance exhibits a steplike decrease associated with a depopulation of the Landau levels. When the normal reflection is increased, the conductance exhibits a sinusoidal oscillation that resembles the Shubnikov–de Haas oscillation in the four-terminal resistance. We find that the conductance becomes maximum near the depopulation threshold of the Landau levels. When the Landau energy $\hbar\omega_c$, where $\omega_c = eB/m$ is the cyclotron frequency, is comparable to μ , periodic resonances show up in the conductance. The emergence of this oscillation does not rely on the normal reflection at the NS interface. We examine the distribution of the current to explore the origin of the resonance states.

II. CALCULATION OF THE TWO-TERMINAL CONDUCTANCE

Consider a wire, defined in $-W/2 < y < W/2$, which consists of 2DEG ($x < 0$) and superconductor ($x > 0$) segments. The phase coherent transmission of the quasiparticle excitations is described by the Bogoliubov–de Gennes equation

$$\begin{pmatrix} H_0 & \Delta(x,y) \\ \Delta^*(x,y) & -H_0^* \end{pmatrix} \begin{pmatrix} u \\ v \end{pmatrix} = \varepsilon \begin{pmatrix} u \\ v \end{pmatrix}, \quad (1)$$

where $u(x,y)$ and $v(x,y)$ are the wave functions of the quasiparticles. The single-particle Hamiltonian is

$$H_0 = [p - eA(x,y)]^2/2m + U(x,y) - \mu, \quad (2)$$

where A and U are the vector and scalar potentials, respectively. For simplicity, we neglect the self-consistency of the pair potential Δ ,⁹ and assume that $\Delta = \Delta_0$ in the superconductor and 0 in the semiconductor. The step-function model is valid when the wire width W is small compared to the superconducting coherence length $\xi = \hbar v_F / (2\Delta)$ (which represents the size of the Cooper pair), or when the resistivity of the semiconductor is larger than the normal resistivity of the superconductor.¹⁰ Throughout this paper, we set Δ_0 to be 2% of the Fermi energy in the 2DEG. This value corresponds to that deduced in the experiment by Takayanagi and Akazaki.⁸ The condition $\xi > W$ to justify the step-function model is satisfied when $k_F W / \pi < 50/\pi$. The magnetic field is assumed to be present only in the 2DEG region. This model corresponds to the situation where the field is completely excluded from the superconductor by the Meissner effect. In this case, a large current supported by a gradient of the order parameter must flow at the edge of the superconductor for the small penetration depth. Experimentally, type-II superconductors are typically utilized to maintain the superconductivity in high magnetic fields. The field partially penetrates the superconductor in the form of thin flux tubes. The conclusions of this paper, at least qualitatively, hold in either case, since nonuniformities in Δ on length scales smaller than ξ do not alter the dynamics of the quasiparticles. It should be emphasized that we focus most of our attention to the zero-bias conductance, and so the conductance of the system is primarily determined by the transport properties of the quasiparticles in the normal region.⁴

When the pair potential is zero, the electronlike and holelike excitations are decoupled. If we choose the vector potential to be $A = (0,0,0)$ for $x \geq 0$ and $A = (0, Bx, 0)$ for $x < 0$, the wave function in the normal region when an electronlike excitation is injected into the NS junction through mode n is given by

$$\begin{aligned} \Psi_n^N(x,y) &= \begin{pmatrix} 1 \\ 0 \end{pmatrix} e^{ik_n^+ x} f_n(y) \exp\left(i \frac{eB}{\hbar} xy\right) \\ &+ \sum_l A_{ln} \begin{pmatrix} 1 \\ 0 \end{pmatrix} e^{-ik_l^+ x} g_l(y) \exp\left(i \frac{eB}{\hbar} xy\right) \\ &+ \sum_l B_{ln} \begin{pmatrix} 0 \\ 1 \end{pmatrix} e^{ik_l^- x} h_l(y) \exp\left(-i \frac{eB}{\hbar} xy\right). \end{aligned} \quad (3)$$

When $B=0$, the wave number and the transverse wave function, respectively, become

$$k_l^\pm = \sqrt{\frac{2m(\mu \pm \varepsilon)}{\hbar^2} - \left(\frac{l\pi}{W}\right)^2}, \quad (4)$$

$$f_l(y) = g_l(y) = h_l(y) = \sqrt{\frac{2}{W}} \sin\left\{\frac{l\pi}{W}\left(y + \frac{W}{2}\right)\right\} \equiv \chi_l(y). \quad (5)$$

We emphasize that the direction of the magnetic field acting on the electronlike and holelike excitations is opposite. Therefore, the edge states that propagate in the same direction are shifted toward the same boundary of the wire. In the superconductor, the wave function is

$$\begin{aligned} \Psi_n^S(x,y) &= \sum_l C_{ln} \begin{pmatrix} \alpha_+ \\ \beta_+ \end{pmatrix} e^{iq_l^+ x} \chi_l(y) \\ &+ \sum_l D_{ln} \begin{pmatrix} \alpha_- \\ \beta_- \end{pmatrix} e^{-iq_l^- x} \chi_l(y), \end{aligned} \quad (6)$$

where the wave number is given by

$$\frac{\hbar^2}{2m} q_l^{\pm 2} = \mu - \frac{\hbar^2}{2m} \left(\frac{l\pi}{W}\right)^2 \pm i\sqrt{\Delta_0^2 - \varepsilon^2}. \quad (7)$$

When the excitation energy ε is below the superconducting gap Δ_0 , the single-particle excitations decay in the superconductor. In this case, we have

$$\alpha_+ = \alpha_- = 1/\sqrt{2}, \quad (8a)$$

$$\beta_+ = \beta_-^* = \frac{\varepsilon - i\sqrt{\Delta_0^2 - \varepsilon^2}}{\sqrt{2}\Delta_0}. \quad (8b)$$

On the other hand, the single-particle excitations are transmitted through the superconductor when $\varepsilon > \Delta_0$. The wave function is written in the well-known form $\alpha_+ = \beta_- = u_0$ and $\alpha_- = \beta_+ = v_0$, with

$$u_0^2 = \frac{1}{2} \left(1 + \frac{\sqrt{\varepsilon^2 - \Delta_0^2}}{\varepsilon}\right) = 1 - v_0^2. \quad (9)$$

The amplitude of the modes A_{ln} , B_{ln} , C_{ln} , and D_{ln} is determined by the continuity of the wave function and its normal derivative.

By virtue of the current conservation, the current can be evaluated in the normal region and is given, within the approximation by Blonder, Tinkham, and Klapwijk, as^{5,11}

$$\begin{aligned} I(V) &= \frac{2e^2}{h} \sum_{l,n} \int_{-\infty}^{\infty} [f_0(\varepsilon - eV) - f_0(\varepsilon)] \\ &\times [1 - R_{ee,ln} + R_{he,ln}] d\varepsilon, \end{aligned} \quad (10)$$

where f_0 is the distribution function. The reflection probabilities are related to the amplitude of the backscattered modes as

$$R_{ee,ln} = (v_l^+ / v_n^+) |A_{ln}|^2, \quad (11a)$$

$$R_{he,ln} = (v_l^- / v_n^+) |B_{ln}|^2, \quad (11b)$$

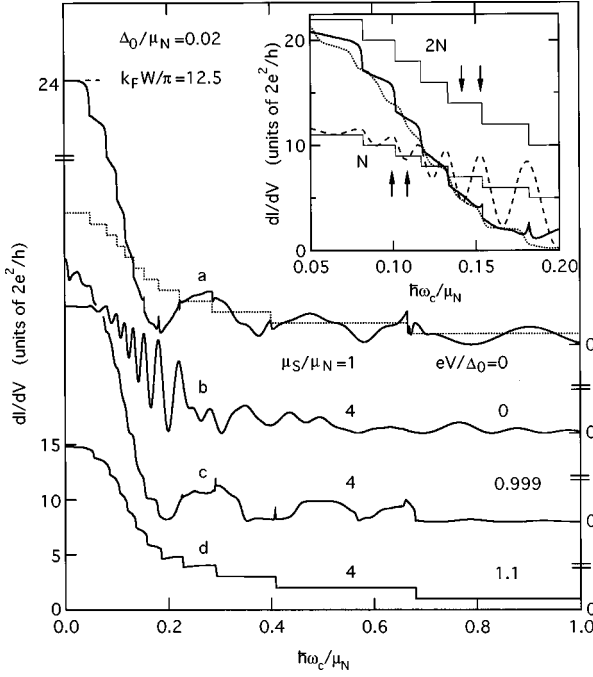


FIG. 1. Differential conductance as a function of magnetic field. The number of modes N when $V=0$ is indicated by the dotted line. The dashed line indicates the conductance value expected when the Andreev reflection is perfect, $24 \times 2e^2/h$. Curves a - c are shown with an expanded scale in the inset by solid, dashed, and dotted lines, respectively. Thin solid lines show N and $2N$. The arrows indicate the magnetic fields for which the bias dependence is calculated in Fig. 4.

where v_l^\pm is the velocity of channel l . Note that the probability conservation requires⁵

$$\sum_l [R_{ee,ln} + R_{he,ln} + (u_0^2 - v_0^2)(T_{ee,ln} + T_{he,ln})] = 1, \quad (12)$$

where the transmission probabilities $T_{ee,ln}$ and $T_{he,ln}$, which become relevant when $\varepsilon > \Delta_0$, are defined as in Eq. (11). Using $R_{ee,ln}$ and $R_{he,ln}$ evaluated at $\varepsilon = eV$, the differential conductance at $T=0$ K is given by the Takane-Ebisawa formula¹²

$$G(V) \equiv \frac{\partial I}{\partial V} = \frac{2e^2}{h} \left(N - \sum_{l,n} R_{ee,ln} + \sum_{l,n} R_{he,ln} \right), \quad (13)$$

where N is the number of incident modes.

III. MAGNETOCONDUCTANCE OF NS JUNCTIONS

Figure 1 shows the differential conductance as a function of the magnetic field. Note that $2\mu_N/\hbar\omega_c$ roughly corresponds to the Landau-level filling factor, where the factor 2 is the spin degeneracy. For curve a , the Fermi energy $\mu_N = \hbar^2 k_F^2/2m$ in the 2DEG is chosen to be identical to that in the superconductor, μ_S . The quasiparticles are almost perfectly Andreev reflected, resulting in the quantization of the zero-field conductance in units of $4e^2/h$.^{13,14} When the number of propagating modes (dotted line) changes with increasing magnetic field, the conductance drops abruptly. Although

the quantization of the conductance in narrow wires of normal conductors is improved in magnetic fields,¹⁵ the quantization in the NS system rapidly deteriorates, indicating the breakdown of the retroproperty by magnetic fields. For $\hbar\omega_c > 0.2\mu_N$, the conductance exhibits an oscillation whose period is unrelated to the magnetic depopulation of the subbands. Due to overlap of the contributions from different modes, the oscillation shows fluctuations when multiple modes are occupied. In the single-mode regime, the conductance vanishes completely at the minima. We also find that the dip is Lorentzian shaped. It is therefore suggested that the high-field oscillation originates from transmission resonance through quasibound states, which are plausibly induced around the NS interface by the magnetic field.¹⁶ On the other hand, the conductance does not reach $4e^2/h$ at the maxima. Moreover, the peak value is suppressed for larger magnetic fields.

The normal reflection is increased for curve b by increasing μ_S relative to μ_N . The steplike structure at low magnetic fields changes to a SdH-like oscillation.^{8,17} The oscillation amplitude increases when the normal reflection is enhanced by increasing the ratio of the Fermi energies. It has been shown that the two-terminal conductance of normal conductors develops dips near the mode thresholds when a disorder is introduced into the system.¹⁸ This is because of the strong scattering due to the long duration time for energies just above the thresholds, and to the quasibound states induced by the impurities for energies just below the thresholds. In contrast to the behavior expected for a 2DEG, the conductance becomes maximum at the depopulation threshold of the Landau levels in the NS system. (Note that no disorder is introduced in Fig. 1.) In high magnetic fields, the conductance oscillation is again unrelated to the subband depopulation. Although the normal reflection seems to be irrelevant to the existence of the high-field oscillation, the period and the peak height critically depend on the normal-reflection probability. We later examine the dependence on the normal-reflection probability in more detail. The Andreev-reflection probability becomes almost unity when the bias applied to the NS junction approaches the superconducting gap. Curve c , for which $eV = 0.999\Delta_0$, hence resembles curve a despite the nonuniform Fermi energy. As the wavelength for the electronlike and holelike excitations is not identical when $V \neq 0$, the number of the steps doubles. When the bias is larger than the gap, the single-particle excitations can propagate in the superconductor. The conductance shown by curve d exhibits a step structure with the height of $2e^2/h$, which is typical in normal conductors. The quantization becomes almost perfect in high magnetic fields. We find that the deficit in the current due to the normal reflection is exactly compensated by the Andreev reflection.¹⁹ Thus the nearly complete quantization of the conductance does not necessarily mean the absence of the reflection in the NS system.

The conductance oscillation is shown in Fig. 2 for three wire widths. The high-field oscillation shows clear single periodicity when only the lowest Landau level is occupied. The period becomes smaller for wider wires. The critical magnetic field for the transition between the two types of oscillation is smaller for wider wires. Therefore, we can expect the low-field conductance to exhibit an additional oscillation while an individual Landau level is being depopulated

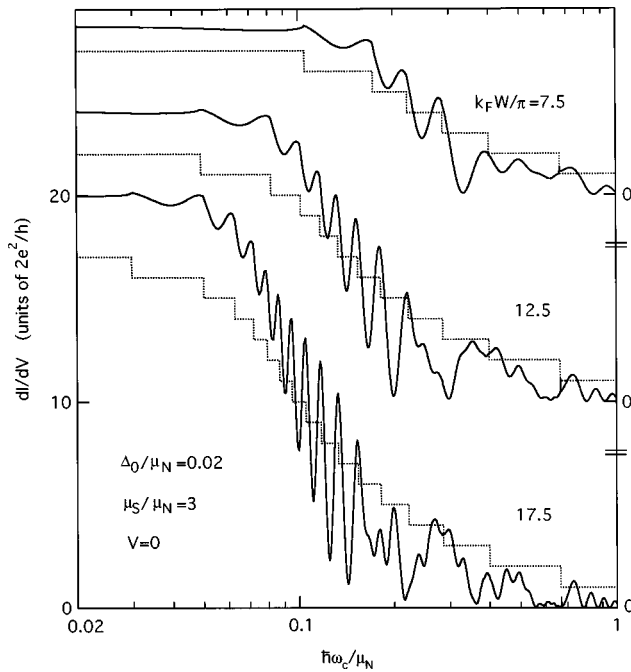


FIG. 2. Differential conductance for three widths of the wire. Dotted lines indicate the number of modes N when $V=0$.

if the wire width is sufficiently large compared to the Fermi wavelength.⁸ In this regime, however, the oscillation would be fairly irregular, in particular for wider wires, due to the overlap of oscillations generated by the multiple modes. When $W > \xi$, the pair potential can no longer be treated as uniform. The phase shift associated with the Andreev reflection acquires a fluctuation, which will result in a suppression of the resonance effect. At finite temperatures, the effective wire width is anticipated to be limited by the phase coherence length.

The conductance reveals a periodic oscillation when W is varied in the single-mode regime. We find that the period δW crucially depends on the magnetic field and the ratio μ_S/μ_N of the Fermi energies (Fig. 3). When $\hbar\omega_c < (>) \mu_N$, the period δW is smaller (larger) for larger μ_S/μ_N . The period becomes nearly independent of μ_S/μ_N when $\hbar\omega_c = \mu_N$.

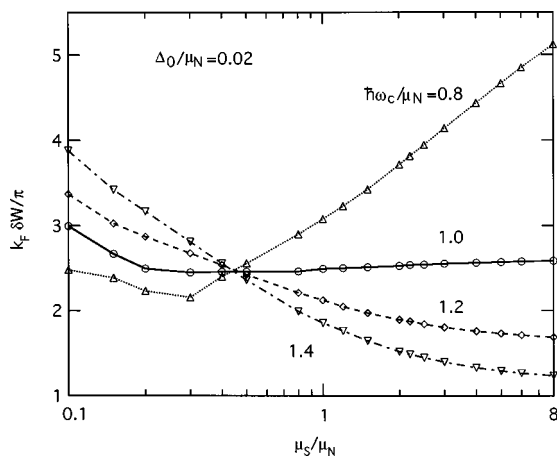


FIG. 3. Period δW of transmission resonance in the single-mode regime.

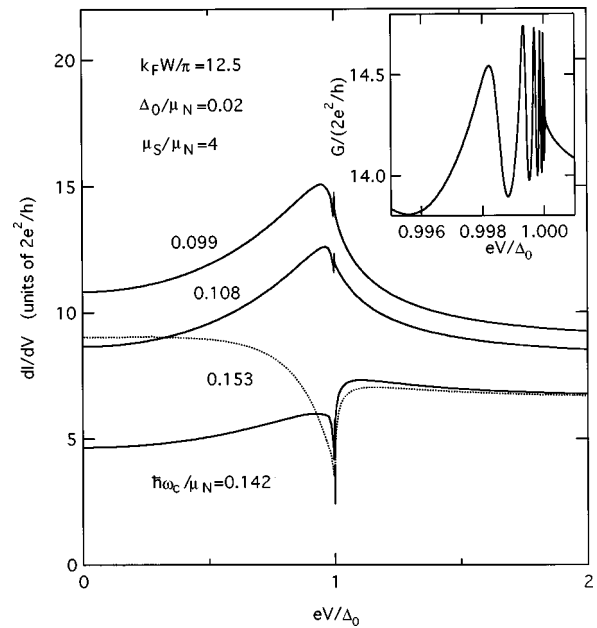


FIG. 4. Bias dependence of the differential conductance for the magnetic fields indicated in the inset of Fig. 1. The inset shows a rapid oscillation at $eV \sim \Delta_0$ for $\hbar\omega_c/\mu_N = 0.099$.

We calculated the bias dependence of the differential conductance (Fig. 4) for the magnetic fields indicated by the arrows in the inset of Fig. 1. The conductance when the Andreev-reflection probability is nearly unity decreases more quickly with increasing magnetic field than it does when the normal-reflection probability is large. Therefore, one can define two regimes using the magnetic field at which the curves cross. In the low-field regime, the conductance always increases when eV approaches Δ_0 due to the enhanced Andreev reflection. On the other hand, the three curves compared in the inset of Fig. 1 roughly take the same value at the minima of the sinusoidal oscillation in the high-field regime. Correspondingly, the broad peak at $eV \approx \Delta_0$ is found to turn into a sharp dip in Fig. 4. Because of the interference effect resulting from the bias-induced breakdown of the retroproperty, a rapid oscillation appears in the conductance when eV

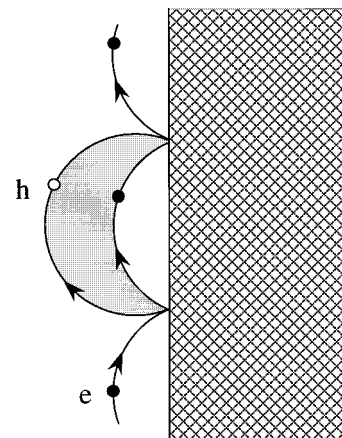


FIG. 5. Classical trajectory of quasiparticle excitations in the presence of a magnetic field. Filled and open circles represent the electronlike and holelike excitations, respectively. The superconducting region is indicated by the hatched area.

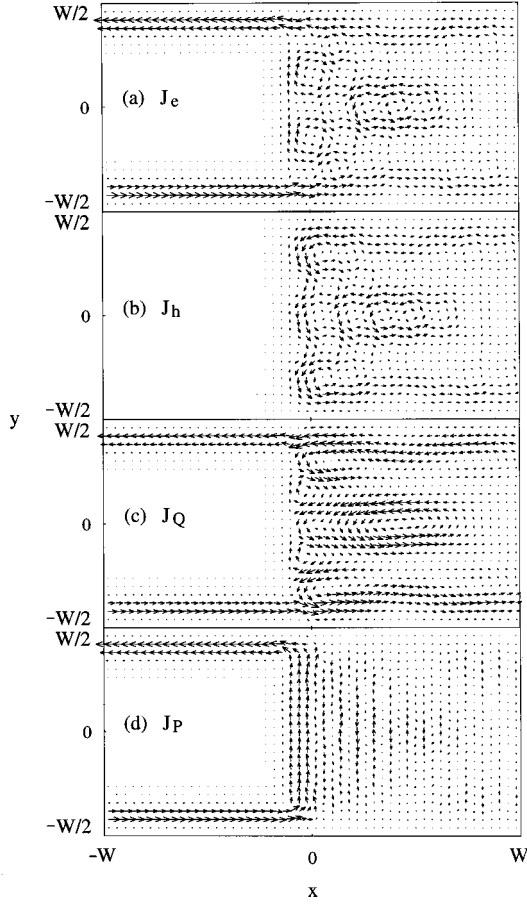


FIG. 6. Distribution of equilibrium current carried by (a) electronlike and (b) holelike excitations for a minimum of the conductance, $G=0$, at $\hbar\omega_c/\mu_N=1.047$. An electronlike excitation is incident from the lower-left corner. Total current density and probability density are shown in (c) and (d), respectively. The length of the arrows in (a) and (b) is normalized using a common factor. Here $k_F W/\pi=7.5$, $\mu_S=\mu_N$, and $V=0$.

is near Δ_0 .⁷ The oscillation begins at smaller values of eV/Δ_0 when Δ_0/μ_N is increased as the difference in the wavelengths of the electronlike and holelike excitations becomes larger.

IV. CURRENT DISTRIBUTION

In terms of the classical trajectory, the reflection of the quasiparticles from the NS interface is described as illustrated in Fig. 5. Let us restrict our discussion to the case of $V=0$. If the Andreev reflection is perfect, the incident quasiparticle changes from one type of excitation to the other after each reflection. When the quasiparticle eventually reaches the boundary at the other side of the wire, it returns to the reservoir connected to the normal wire through either the electron or the hole channels. The conductance will thus oscillate when the wire width is varied by an amount which is roughly given by the cyclotron diameter $l_c=2\hbar k_F/eB$. A close relation of this classical trajectory to the high-field oscillation is suggested by the distribution of the current.

In Figs. 6 and 7, we show the current density defined by

$$J_Q(x,y)=J_e(x,y)+J_h(x,y), \quad (14)$$

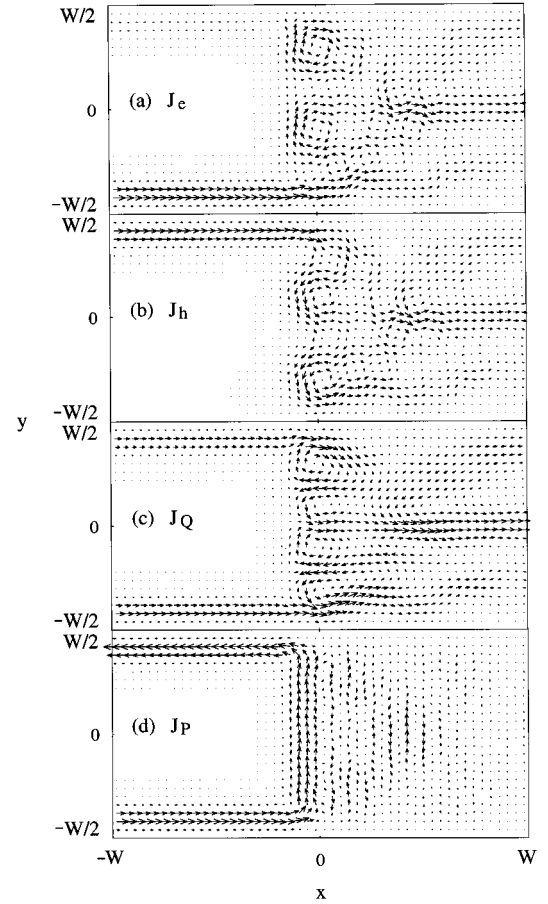


FIG. 7. Distribution of equilibrium current carried by (a) electronlike and (b) holelike excitations for a maximum of the conductance, $G=1.75\times 2e^2/h$, at $\hbar\omega_c/\mu_N=0.82$. An electronlike excitation is incident from the lower-left corner. Here $k_F W/\pi=7.5$, $\mu_S=\mu_N$, and $V=0$.

where the currents J_e and J_h carried, respectively, by the electronlike and holelike excitations, are given by

$$J_e(x,y)=\frac{e\hbar}{m}\text{Im}(u^*\nabla u)-\frac{e^2}{m}A|u|^2, \quad (15a)$$

$$J_h(x,y)=\frac{e\hbar}{m}\text{Im}(v^*\nabla v)+\frac{e^2}{m}A|v|^2. \quad (15b)$$

The current density satisfies the continuity equation

$$\nabla\cdot J_Q=(4e/\hbar)\text{Im}(\Delta u^*v). \quad (16)$$

One can also define the probability density

$$J_P(x,y)=[J_e(x,y)-J_h(x,y)]/e, \quad (17)$$

for which the conservation law is given by

$$\nabla\cdot J_P=0. \quad (18)$$

In the normal side of the NS junction, the current is carried by the electronlike and holelike excitations alternately after successive reflections. For Figs. 6 and 7, l_c/W in the normal region is estimated, respectively, to be 0.16 and 0.21. These values roughly correspond to the diameter of the current loop at the interface. When W is an even-integer multiple of the

loop diameter, the quasiparticle leaves the system through the electron channels, giving rise to the conductance minima.

We notice that the period plotted in Fig. 3 possesses a universality $(k_F \delta W / \pi)(\hbar \omega_c / \mu_N) \approx 2.51$ at $\mu_S \approx \mu_N$. This value is in excellent agreement with the one $(8/\pi)$ expected when $\delta W = 2l_c$. The amplitude of the high-field oscillation decreases drastically when the normal reflection becomes stronger as the alternate arrival of the electronlike and holelike excitations is obscured. We also notice that the transition magnetic field between the two regimes is well described by a condition $2l_c \approx W$, indicating that the quasiparticles are multiply reflected from the NS interface in the high-magnetic-field regime. These observations are consistent with the classical interpretation. However, this mechanism does not anticipate the complete disappearance of the conductance. Although the detail is not clear at the moment, the quantum-mechanical effect in the superconductor is expected to have produced the quasibound states. We emphasize that the current distributions for the minima and the maxima of the conductance are remarkably similar. This is unexpected since the current distribution at the resonance condition (Fig. 6) would reflect the standing wave pattern of the probability distribution of the quasibound state.

Note that, despite the absence of the magnetic field, vortices are created in the superconductor region. Such vortices when $B=0$ were reported to appear in a nonuniform interacting system as a consequence of the gauge field.²⁰ The circular vortices in the electron and the hole current are canceled in the total current distribution in such a way that elliptic vortices are left. The flow of the probability current in the superconductor stirred by the edge state in the 2DEG is relaxed by creating a chain of vortices and antivortices. For comparison, we also examined the current distribution in a 2DEG wire with a constant width. The magnetic field is similarly assumed to be B for $x < 0$ and 0 for $x > 0$. The incident edge state is totally reflected by placing a barrier potential $U (\geq \mu_N)$ in the region of $x > 0$ instead of the superconductor. In this case, however, we did not find the vortices in the barrier region (not shown).²¹

We point out that the skipping orbit along the NS interface can give rise to an Aharonov-Bohm (AB)-type interference effect when the normal reflection probability is non-zero. Suppose that an electronlike excitation remains to be an electronlike excitation after two consecutive reflections from the NS interface. If the Andreev reflection is not perfect, there are two possibilities for this to happen: two Andreev reflections or two normal reflections. The phase difference between these two probability amplitudes is modulated by the magnetic field, and this leads to a conductance oscillation. This interference effect may be the origin of the μ_S/μ_N dependence of the period in Fig. 3. The phase shift is obtained by the line integral of the wave number and the vector potential along the trajectory. It can be shown that, between the electron and hole paths, the phase shift due to the wave number adds constructively, whereas that due to the vector potential adds destructively. This is opposite to the phase cancellation for the Andreev-reflected trajectory.²² Therefore, the phase accumulation is given by

$$\delta\theta = \pi k_F l_c + 2\pi\phi/\phi_0 + \theta_0, \quad (19)$$

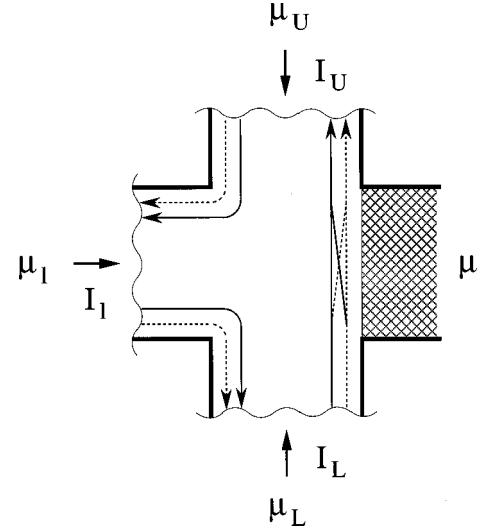


FIG. 8. Edge-state configuration in four-terminal NS junction. The superconductor lead is indicated by the hatched region. The solid and dotted lines represent the edge states of the electronlike and holelike excitations. μ_i is the chemical potential of the reservoir i , and I_i is the current.

where ϕ is the magnetic flux that threads through the area enclosed by the electron and hole trajectories (shaded area in Fig. 5), $\phi_0 = h/e$, and θ_0 is the phase shift arising from the reflection. The phase shift due to the wave number is independent of the center coordinate of the cyclotron orbit. The AB flux ϕ , on the other hand, depends on the center coordinate, and is zero if the orbit center is located at the interface. Further studies are hence required to find out if the phase modulation survives after all contributions with various phase shifts, due to different center coordinates and reflection history, are added up.

V. HALL RESISTANCE IN NS JUNCTIONS

Finally, let us consider the Hall resistance in NS junctions. The current flows across the NS junction horizontally, while the Hall voltage is measured between the upper and lower leads in Fig. 8. We choose the polarity of the magnetic field to be $\mu_L > \mu > \mu_U$. Therefore, electronlike excitations with energies between μ_L and μ are injected into the cross junction from the lower lead, whereas holelike excitations with energies between μ and μ_U are injected from the upper lead. The current in the normal leads is evaluated using the Lambert formula,²³ which extended Büttiker's approach²⁴ to the NS system. We restrict our discussion to the zero-bias resistance. At $\varepsilon=0$, the group velocities of the electronlike and holelike excitations are equal to the Fermi velocity. Hence, the current I_l , for instance, is given at $T=0$ by

$$I_l = (2e/h)[(N - R_{ee}^l + R_{he}^l)(\mu_l - \mu) - (T_{ee}^{lL} - T_{he}^{lL})(\mu_L - \mu) - (T_{eh}^{lU} - T_{hh}^{lU})(\mu - \mu_U)], \quad (20)$$

where $R_{\rho\sigma}^l$ is the reflection probability in the left-hand side lead for quasiparticles of type σ to quasiparticles of type ρ and $T_{\rho\sigma}^{ij}$ the transmission probability for quasiparticles of type σ in lead j to quasiparticles of type ρ in lead i . As suggested in Figs. 6 and 7, the quasiparticles injected from

the left-hand side (upper) lead will be totally transmitted into the same type of the quasiparticles in the lower (left-hand side) lead when the edge states are well-established. The expression for the current, thus, reduces to

$$I_I = (2e/h)[N(\mu_I - \mu) + N(\mu - \mu_U)], \quad (21a)$$

$$I_L = (2e/h)[N(\mu_L - \mu) - N(\mu_I - \mu)], \quad (21b)$$

$$I_U = (2e/h)[-N(\mu - \mu_U) + (T_{\text{he}}^{UL} - T_{\text{ee}}^{UL})(\mu_L - \mu)]. \quad (21c)$$

Imposing the conditions for the Hall resistance measurement, $I_I = I$ and $I_L = I_U = 0$, we find that the Hall resistance is

$$R_H \equiv e(\mu_L - \mu_U)/I = h/(2e^2N). \quad (22)$$

In contrast to the doubling effect in the two-terminal conductance,¹³ the Hall resistance is not affected by the Andreev reflection from the NS interface, provided that the magnetic field is in the Hall plateau region. Similarly, we find that the Hall resistance is also given by Eq. (22) when the current flows in the vertical direction. Note that, at weak magnetic fields or in the transition regions between the Hall plateaus, the Hall resistance is expected to be modified significantly by the Andreev reflection.

The independence of R_H on the Andreev reflection probability is reminiscent of the independence of R_H on the partial reflection of the edge states in gated cross junctions of normal conductors. The Hall resistance in normal cross junctions is unaffected when higher-lying edge states are reflected by a potential barrier in one of the leads. However, when the edge states are partially reflected in two adjacent leads, R_H is determined by the number of transmitted edge states rather than the filling factor in the bulk region.^{25,26} We therefore expect the influence of the Andreev reflection to show up in R_H when the number of transmitted edge states is decreased in the upper lead by a gate. Analyzing the Lambert formula, we indeed find that

$$R_H = \frac{h}{2e^2} \frac{T_{\text{ch}}^{UL}}{K(T_{\text{ch}}^{UL} + T_{\text{ch}}^{LL})}, \quad (23)$$

where the lowest K edge states are assumed to be transmitted through the upper lead. In the adiabatic limit, the Andreev-reflected quasiparticles are transmitted into the upper lead by the K lower-lying edge states and into the left-hand side lead by the $N-K$ higher-lying edge states. Notice that $T_{UL}^{\text{ch}} + T_{LL}^{\text{ch}}$ is the total Andreev reflection probability and is independent of the gate voltage. Although the absolute value of the Andreev reflection probability cannot be determined, the distribution of the Andreev-reflected quasiparticles among the edge states can be estimated from the plateau value of R_H for various values of K . It is noteworthy that, in contrast to the case of the selective injection and detection of the edge states in the normal conductors, R_H is given by the filling factor in the bulk region, Eq. (22), when the distribution is uniform.

VI. SUMMARY

In conclusion, we have investigated the magnetotransport properties in NS junctions. We find that the conductance exhibits two types of oscillation for low and high magnetic fields. The low-field oscillation is associated with the depopulation of the Landau levels. The conductance decreases in a steplike manner when the Andreev reflection is almost perfect, whereas the shape changes to a sinusoidal oscillation when the normal-reflection probability is increased. In high magnetic fields, Lorentzian-shaped dips appear periodically when the ratio of the wire width and the cyclotron diameter is varied. Evidence indicates that the high-field oscillation originates from the skipping orbit along the NS interface. We have also shown that the Hall resistance in the NS junction is not affected by the quasiparticle reflection from the NS interface when the interboundary edge state scattering is absent. The plateau value is influenced by the Andreev reflection when higher-lying edge states in the voltage lead are reflected by a gate. The distribution of the Andreev-reflected quasiparticles among the edge states can be determined by the selective detection technique.

ACKNOWLEDGMENTS

The author gratefully acknowledges helpful discussions with Y. Tokura, H. Takayanagi, H. Nakano, and C. J. P. M. Harmans.

¹B. J. van Wees, P. de Vries, P. Magnée, and T. M. Klapwijk, Phys. Rev. Lett. **69**, 510 (1992).
²H. Takayanagi and T. Akazaki, Phys. Rev. B **52**, 8633 (1995); Jpn. J. Appl. Phys. **34**, 6977 (1995).
³A. F. Andreev, Zh. Eksp. Teor. Fiz. **46**, 1823 (1964) [Sov. Phys. JETP **19**, 1228 (1964)].
⁴C. W. J. Beenakker, in *Mesoscopic Quantum Physics*, edited by E. Akkermans, G. Montambaux, and J.-L. Pichard (North-Holland, Amsterdam, 1995).
⁵G. E. Blonder, M. Tinkham, and T. M. Klapwijk, Phys. Rev. B **25**, 4515 (1982).
⁶M. Leadbeater and C. J. Lambert, Phys. Rev. Lett. **74**, 4519 (1995).
⁷Y. Takagaki and Y. Tokura, Phys. Rev. B **54**, 6587 (1996).
⁸H. Takayanagi and T. Akazaki (unpublished).
⁹J. Sánchez-Cañizares and F. Sols, Phys. Rev. B **55**, 531 (1997).

¹⁰K. K. Likharev, Rev. Mod. Phys. **51**, 101 (1979).
¹¹C. J. Lambert, J. Phys. Condens. Matter **3**, 6579 (1991).
¹²Y. Takane and H. Ebisawa, J. Phys. Soc. Jpn. **61**, 1685 (1992).
¹³C. W. J. Beenakker, Phys. Rev. B **46**, 12 841 (1992).
¹⁴Y. Takagaki and H. Takayanagi, Phys. Rev. B **53**, 14 530 (1996).
¹⁵C. W. J. Beenakker and H. van Houten, Phys. Rev. B **39**, 10 445 (1989).
¹⁶Y. Takagaki and K. Ploog, Phys. Rev. B **51**, 7017 (1995).
¹⁷A. F. Morpurgo, S. Holl, B. J. van Wees, T. M. Klapwijk, and G. Borghs, Phys. Rev. Lett. **78**, 2636 (1997).
¹⁸P. F. Bagwell, Phys. Rev. B **41**, 10 354 (1990).
¹⁹T. Ando, Phys. Rev. B **44**, 8017 (1991).
²⁰M. Rasolt and F. Perrot, Phys. Rev. Lett. **69**, 2563 (1992).
²¹T. Ohtsuki and Y. Ono, J. Phys. Soc. Jpn. **59**, 637 (1990).
²²P. W. Brouwer and C. W. J. Beenakker, Phys. Rev. B **52**, 3868 (1995).

- ²³C. J. Lambert, V. C. Hui, and S. J. Robinson, *J. Phys. Condens. Matter* **5**, 707 (1993).
- ²⁴M. Büttiker, *IBM J. Res. Dev.* **32**, 317 (1988).
- ²⁵B. J. van Wees, E. M. M. Willems, C. J. P. M. Harmans, C. W. J. Beenakker, H. van Houten, J. G. Williamson, C. T. Foxon, and J. J. Harris, *Phys. Rev. Lett.* **62**, 1181 (1989).
- ²⁶M. Büttiker, in *Nanostructured Systems*, edited by M. Reed (Academic, San Diego, 1992), p. 191.